ORIGINAL ARTICLE

Volume 19 Issue 2 2024

DOI: 10.21315/aos2024.1902.OA07

ARTICLE INFO

Submitted: 11/06/2023
Accepted: 17/11/2024
Online: 23/12/2024

Effect of Change Angulation and Material of Mini-screw Inserted in Retromolar Pad Area on Stress Distribution: A Finite Element Simulation Study

Nada Nashee Al-Hafidh[a*], Saeed AlSamak[a], Mohammed T. Sulaiman Al-Abbood[b], Ali R. Al-Khatib[a]

[a]*Department of Paedodontics, Orthodontics and Preventive Dentistry, College of Dentistry, University of Mosul, Mosul 41002, Iraq*

[b]*Department of Mechanical Engineering, College of Engineering, University of Mosul, Mosul 41002, Iraq*

[*]Corresponding author: nadanashee@uomosul.edu.iq

To cite this article: Al-Hafidh NN, AlSamak S, Al-Abbood MTS, Al-Khatib AR (2024). Effect of change angulation and material of mini-screw inserted in retromolar pad area on stress distribution: A finite element simulation study. *Arch Orofac Sci*, **19**(2): 173–186. https://doi.org/10.21315/aos2024.1902.OA07

To link to this article: https://doi.org/10.21315/aos2024.1902.OA07

ABSTRACT

This study evaluated the influence of angulation and material composition on the stress distribution and displacement of mini-screws placed in the retromolar pad area using finite element analysis; these mini-screws inserted in the retromolar pad area were referred to as MRM. A 3D mandible model was generated from CT scan data using Mimics and 3-Matic software, while the mini-screw was modelled in AutoCAD. Finite element analysis was performed with Inventor Professional software. A 2 N force, parallel to the occlusal reference line (ORL), was applied to MRM at insertion angles of 0°, 15°, 30°, 45°, and 60° relative to the ORL. Three MRM materials were analysed: stainless steel (SS), titanium alloy (Ti-6Al-4V), and pure titanium (Ti). Results revealed that the lowest Von Mises stresses occurred at a 0° insertion angle, while the highest stresses were observed at 60°. Stress levels were comparable across materials at 0°, 15°, and 30°, but SS MRM generated higher stresses than titanium materials at 45° and 60°. Displacement analysis indicated that SS MRM had the lowest displacement, while Ti MRM exhibited the highest across all angles. Importantly, all stress values remained below the bone's yield strength, and displacements were clinically insignificant. For optimal stability, a 0° insertion angle is recommended, with 15° and 30° serving as viable alternatives. These findings provide guidance on selecting mini-screw angulation and materials for effective orthodontic anchorage in the retromolar pad area.

Keywords: *Finite element analysis; mini-screw; orthodontics; retromolar pad area; stress distribution*

INTRODUCTION

In recent decades, the use of orthodontic mini-screws has increased in the treatment of various orthodontic cases due to their advantages in providing skeletal anchorage (Papadopoulos & Tarawneh, 2007; Nienkemper *et al.*, 2012; Chandhoke *et al.*, 2015). There are many possible sites for mini-screw placement, including the intra-

and extra-alveolar sites (Baumgaertel & Hans, 2009; Papageorgiou *et al.*, 2012; Al-Hafidh *et al.*, 2020, Al-Hafidh *et al.*, 2022, AlSamak *et al.*, 2022). The insertion of a mini-screw into extra-alveolar sites, such as the infra-zygomatic crest, buccal shelf and mandibular retromolar pad area has been efficiently used in obtaining the skeletal anchorage (Baumgaertel & Hans, 2009; Magkavali-Trikka *et al.*, 2018). Inserted mini-screws in the retromolar (MRM) pad area seem to offer a feasible solution for distalisation of the mandibular dentition in dental class III malocclusion (Poletti *et al.*, 2013; Yeon *et al.*, 2022). It is also used for treating tipped or mesially impacted mandibular molars and open bite cases with a hyper-divergent skeletal pattern (Sugawara *et al.*, 2008; Yanagita *et al.*, 2011; Magkavali-Trikka *et al.*, 2018). Retromolar pad area, situated far from dental roots and characterised by thick and dense cortical bone which provides high primary stability for mini-screw (Park *et al.*, 2008; Wang *et al.*, 2021). Primary stability is obtained by mechanical interdigitation between mini-screws and surrounding bone, and it relies primarily on supporting bone quantity and quality such as bone thickness and bone density (Migliorati *et al.*, 2015). Primary stability is necessary for immediate orthodontic force application on the mini-screw (Migliorati *et al.*, 2012). When orthodontic forces applied on mini-screws including MRM, the force transmitted through the mini-screws to the surrounding bone, and this is referred to as stress distribution. High primary stability led to even stress distribution, however different angulations of mini-screw lead to different pattern of stress distribution (Kuroda *et al.*, 2017). Uneven stress distribution can negatively affect primary stability, as the concentration of stress at certain points at the mini-screw bone interface leads to microdamage to the bone surrounding the MRM at these points (Kuroda *et al.*, 2017). Therefore, angulation is a critical factor in determining the stability of orthodontic mini-screws (Paul *et al.*, 2021). Additionally, if the stress induced by a mini-screw exceeds the physiologic limit, it will probably lead to a microfracture in the bone surrounding the mini-screw and eventually cause necrosis of the bone, ultimately leading to the loosening of the mini-screw (Sivamurthy & Sundari, 2016).

Finite element study is a dependable method to simulate and analyse the stress and displacement that occur in and around mini-screws (Omar *et al.*, 2011; Suzuki *et al.*, 2011; Lee *et al.*, 2013; Perillo *et al.*, 2015; Cozzani *et al.*, 2020; Sidhu *et al.*, 2020). By solving equations for each element and then combining the results, finite element analysis provides detailed insights into how forces are distributed within the structure. Although studies in the literature have measured the effect of different angles of mini-screw insertion on the pattern of stress distribution (Omar *et al.*, 2011; Suzuki *et al.*, 2011; Lee *et al.*, 2013; Perillo *et al.*, 2015; Choi *et al.*, 2016; Cozzani *et al.*, 2020; Sidhu *et al.*, 2020), most of these studies simulated the site of mini-screw insertion as a bone block with hypothetical cylindrical or cuboid models (Suzuki *et al.*, 2011; Lee *et al.*, 2013; Perillo *et al.*, 2015; Cozzani *et al.*, 2020). Moreover, a limited number of studies have relied on clinical data from humans in the simulation of mini-screw insertion sites (Omar *et al.*, 2011, Choi *et al.*, 2016). In fact, only Omar *et al.* (2011) depended on a CT scan to simulate the left maxillary posterior region containing the second premolar and first and second molars. Choi *et al.* (2016) adopted a model that represented a portion of the maxilla with an extracted first premolar obtained by laser scanning of an adult occlusion.

It is important to mention that to the best of our knowledge; no study has addressed the stress distribution generated by mini-screws inserted in the retromolar pad area. While investigation of the effect of mini-screw angulation on hypothetical models can provide an idea about the biomechanical behaviour of mini-screws, accurate simulation of mini-screw insertion sites is mandatory to obtain clinically relevant data, since different anatomy, thickness and

density of bone in the retromolar pad area could affect the pattern of stress distribution in MRM and surrounding bones (Alrbata *et al.*, 2014). For instance, if an MRM was a self-drilling mini-screw and made from brittle material, such as titanium, and inserted in a retromolar pad area, which possesses particularly thick cortical bone, the produced high stresses can make the mini-screw more liable to fracture (Mecenas *et al.*, 2020). This scenario could be different if the clinicians used an MRM made from materials with higher strength and fracture torque, such as stainless steel (Mecenas *et al.*, 2020; Barros *et al.*, 2021). Consequently, this study aimed to determine the optimal angulation of MRM relative to a clinical reference line and investigate stress distribution in and around MRM made of different materials. The null hypothesis assumed that changing the angulation and materials would not change the stress distribution within and around the mini screw.

MATERIAL AND METHODS

Data Acquisition

A three-dimensional (3D) model of the mandible was reconstructed using a CT scan dataset of an 18-year-old healthy adult male. The scan was performed with multi-slice CT (Briliance 64 slice, Philips Company, Amsterdam, Holland). The scanning parameters were set as 120 kV and 80 mAs with an image resolution of 513 × 513 pixels and a slice thickness of 0.8 mm. The scan was saved in digital imaging and communications in medicine (DICOM) format. Since the scan was originally conducted for other medical purposes, the patient was not exposed to additional radiation for this study. This research was conducted according to the principles of the Declaration of Helsinki (WMA, 2013).

3D Modelling

For modelling of the mandible, the DICOM file was imported into Mimics software (version 21.0, Materialise, Leuven, Belgium). The threshold tool was used to segment bone by selecting pixel intensity ranges that correspond to bone tissue in the CT images. This tool isolates the bone from surrounding soft tissues, allowing for more accurate identification of the mandible. After segmentation, the mandible was separated from the maxilla using a split mask (Fig. 1a). The segmented data was imported as a stereo-lithographic file (STL) into 3-Matic software (version 21.0, Materialise, Leuven, Belgium) for further smoothing and wrapping of the model (Fig. 1b).

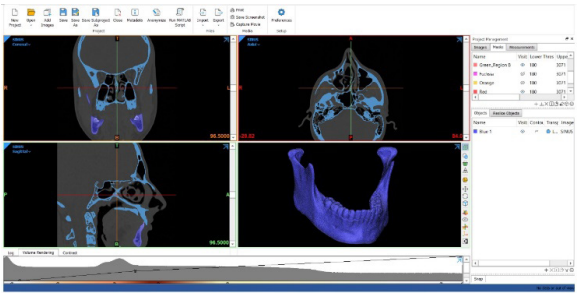

(a)

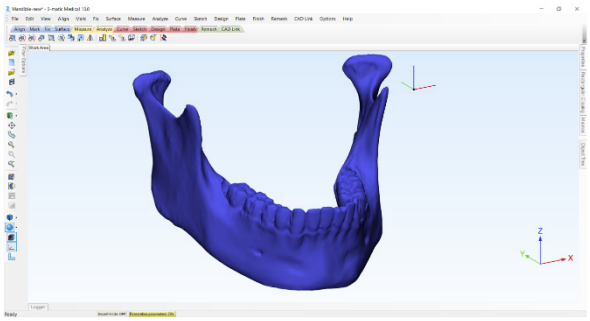

(b)

Fig. 1 (a) Mimic software used for segmentation of the mandible from a CT image; (b) 3-Matic software used for smoothing the mandibular model.

Finite Element Analysis

The 3D model of the mandible was imported into Inventor Professional Software 2023 (Autodesk Inc., 111 Mclnnis Parkway, San Rafael, CA 94,903, USA). To create the mini-screw (MRM) model, AutoCAD Software 2023 was used (Autodesk Inc., 111 Mclnnis Parkway, San Rafael, CA 94, 903, USA). The authors utilised the dimension of MAS MINI-SCREW (Micerium, Avegno GE, Italy) which are 10 mm in length and

2 mm in diameter. Once the MRM model was created, it was imported into Inventor Software for further analysis. To determine the angle for inserting the MRM, a line was drawn to connect the buccal cusp of the second molar with the cusp of the canine in the software. This line, called the occlusal reference line (ORL), is used as a guide to standardise the insertion angle of the MRM (Fig. 2).

In the first test, MRM was inserted at a zero-degree angle parallel to the ORL. Five different models were created in the Inventor software. Each model represents different angles of the MRM (0°, 15°, 30°, 45°, and 60°) relative to the ORL. For each angle, we also tested three different materials of MRM: commercially pure titanium (Ti), titanium alloy (Ti6Al-4V) and stainless steel (SS). The material properties of different MRM materials are illustrated in Table 1.

To simulate how mini-screw behaves when inserted into the bone, the MRM was subtracted from the bone structure to create the three-dimensional space the MRM would occupy later during the simulation. Interaction between the MRM and bone was simulated using a rotational contact. This means that the contact between the mini-screw and the bone allows for some rotational movement. This is important because it mimics the actual physical behaviour of the screw during insertion and under load, providing a more accurate simulation of stress distribution.

Following this, the size of elements was determined based on recommendations from Inventor software, then each assembled model was meshed, meaning it was divided into these recommended elements size to improve the accuracy of the simulation. The number of nodes and elements for each model configuration is detailed in Table 2, demonstrating the mesh density used for the finite element analysis.

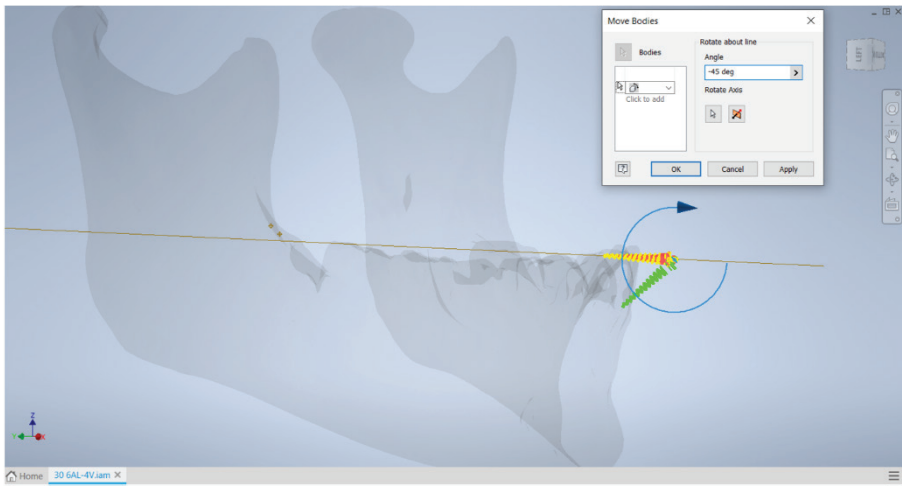

Fig. 2 Occlusal reference line.

Table 1 Properties of the materials

Material	Cortical bone	Stainless steel MRM	Titanium alloy grade 5 MRM	Pure titanium MRM
Poisson's ratio	0.26	0.29	0.32	0.36
Young's modulus	13.7 E+09 Pa	2.05 E+11 Pa	1.138 E+11 Pa	1.028 E+11 Pa

Table 2 Numbers of nodes and elements of each model

No. of nodes/elements	0°	15°	30°	45°	60°
Nodes	4206005	4289527	4267948	4238680	4247301
Elements	2982581	3045731	3029278	3006448	3012911

To simulate the clinical scenario of mandibular dentition's distalisation, a 2 N force was applied to the MRM parallel to the ORL (Suzuki *et al.*, 2011; Alrbata *et al.*, 2014; Perillo *et al.*, 2015). To prevent the mandible from moving freely throughout the simulation, constraints were applied along the three planes of movement, allowing to measure how the bone and MRM behave under the applied force. The material properties of the surrounding bone were assumed to be homogeneous, isotropic and linearly elastic based on previous studies (Carter & Hayes, 1977; Nowak *et al.*, 2021), as shown in Table 1.

RESULTS

The results of finite element analysis represent the distribution of the Von Mises stress across the entire mandible under different loading conditions (Fig. 3a). Von Mises stress is a measure used to predict when a material begins to fail under stress. The lowest values of Von Mises stresses in bone were seen when the angle between the MRM and the ORL was 0°. At this angle, the Von Mises stress values were 5.184 MPa for SS, 5.185 MPa for Ti alloy, and 5.186 MPa for Pure Ti. The highest values of Von Mises stresses were observed at 60° angle, which were 8.812 MPa for SS, 7.710 MPa for Ti alloy, and 7.468 MPa for pure Ti.

For angles of 0°, 15° and 30°, the Von Mises stresses were almost similar for the three MRM materials. However, at angles of 45° and 60°, the SS MRM recorded the highest Von Mises stresses, while pure Ti had the lowest.

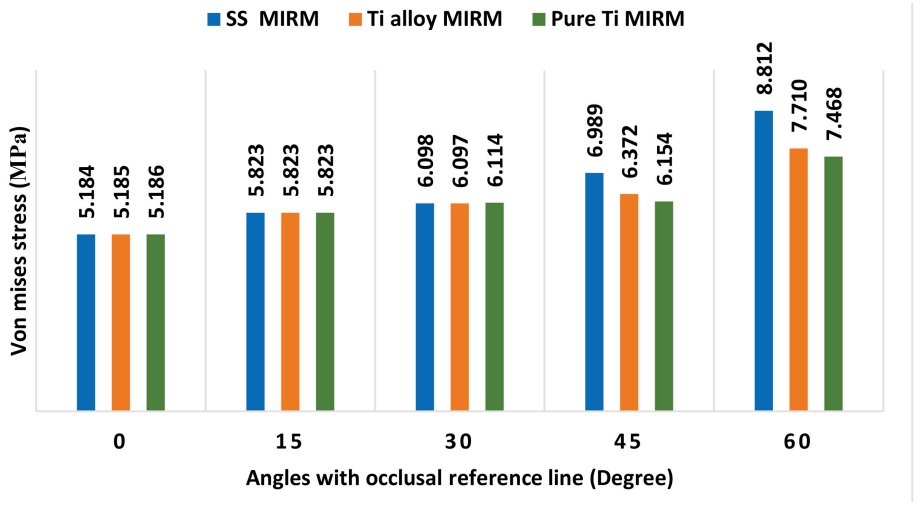

(a)

Fig. 3 (a) Von Mises stresses of SS, Ti alloy, and pure Ti with different angles of MRM. (*continued on next page*)

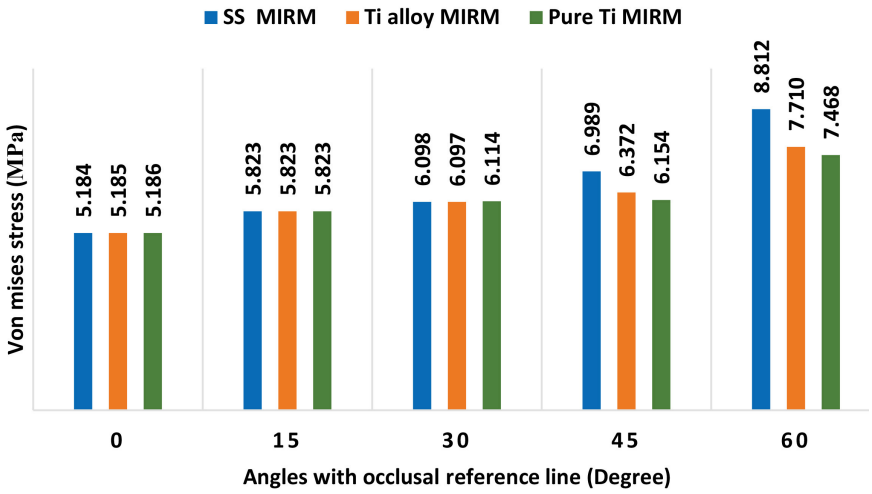

(b)

Fig. 3 (b) Displacements of SS, Ti alloy, and pure Ti with different angles of MRM.

Fig. 3b illustrates the displacement values, which represent how much the MRM move under load at different angles. At an angle of 0°, the smallest displacement values were recorded: 0.3306 µm for SS, 0.3479 µm for Ti alloy, and 0.3517 µm for pure Ti. The highest displacements observed at a 60° angle, with values of 0.5771 µm for SS, 0.6648 µm for Ti alloy, and 0.6843 µm for pure Ti. Across all angles, SS had the smallest displacements, while pure Ti exhibited the largest.

Fig. 4a and 4c illustrate the Von Mises stress distribution using a colour scale, making it easier to see how stress is spread across the mandible. Similarly, Fig. 4b and 4d display the displacement values with a colour scale for a more comprehensive understanding. Additionally, Fig. 5 provides cross-sectional views of the Von Mises stress distribution for the different MRM materials at 60° angle.

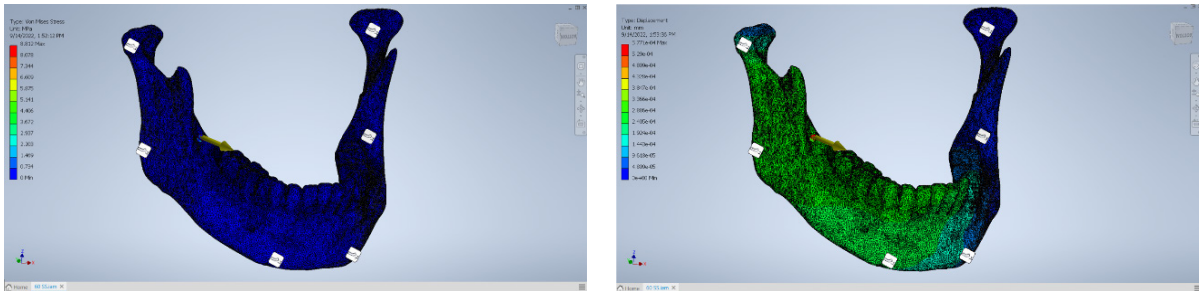

(a) (b)

Fig. 4 (a) Von Mises stress of the SS mini-screw at an angle of 60°; (b) displacement of the SS mini-screw at an angle of 60°; (*continued on next page*)

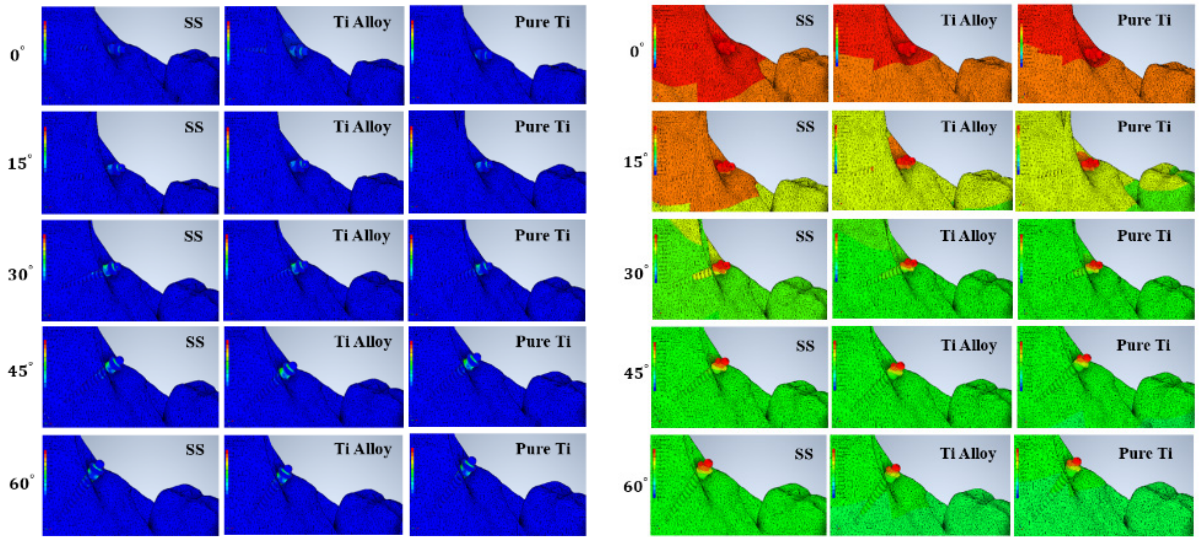

(c) (d)

Fig. 4 (c) Von Mises stresses in the MRM and surrounding bone induced with different materials and at different angulations; and (d) displacements of the MRM and surrounding bone with different materials and at different angulations.

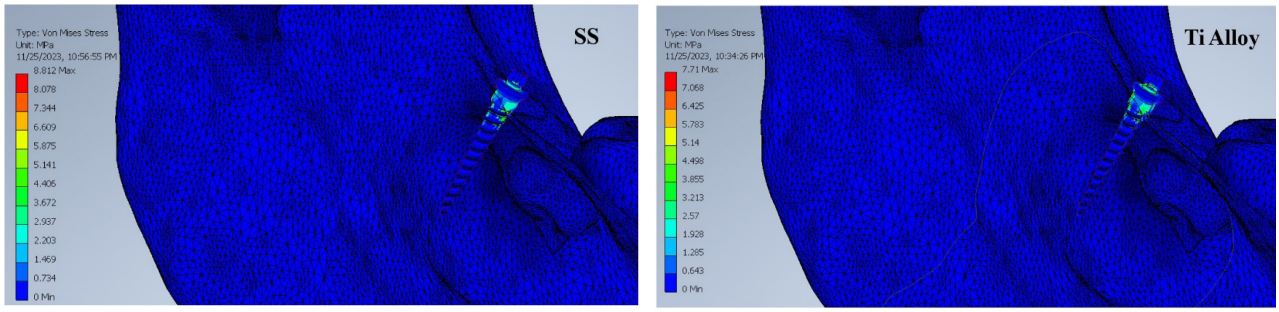

(a) (b)

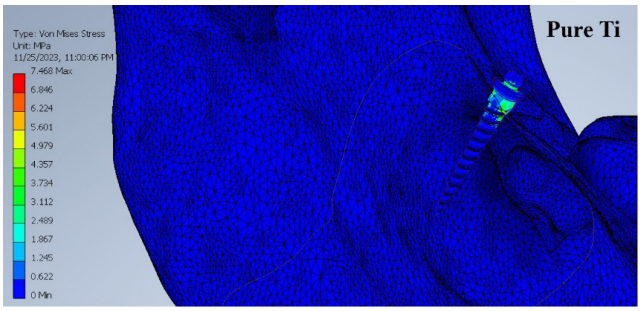

(c)

Fig. 5 Cross-sections of MRM and surrounding bone show Von Mises stress distributions at 60° angle for (a) SS; (b) Ti alloy; and (c) pure Ti.

Table 3 Reliability assessment of stress distribution and displacement in stainless steel MRM across different mesh densities

Von Mises stress distribution (MPa)			
Model angle (degree)	**Element size (fine)**	**Element size (medium)**	**Element size (coarse)**
0°	5.184	5.067	4.072
15°	5.823	5.733	4.445
30°	6.098	6.377	6.098
45°	6.989	6.599	6.848
60°	8.812	8.210	8.095
Displacement (µm)			
Model angle (degree)	**Element size (fine)**	**Element size (medium)**	**Element size (coarse)**
0°	0.3306	0.2557	0.2330
15°	0.3779	0.3041	0.2780
30°	0.4558	0.4871	0.4553
45°	0.5449	0.5708	0.5441
60°	0.5771	0.6166	0.5763

To ensure the reliability of results, a mesh convergence study was conducted for the five angles with stainless steel MRM. Von Mises stresses and displacements were investigated using three different element sizes (coarse, medium and fine) for each angle. As shown in Table 3, stresses and displacements values were consistent across different mesh densities. This behaviour demonstrates the reliability of the simulation results.

DISCUSSION

The results of this study showed that the increase in MRM insertion angle with respect to the ORL was associated with an increase in Von Mises stresses. Furthermore, the SS MRM created higher stresses compared to other materials at 45° and 60° angles.

One of the crucial aims of this study was to create a model that would be representative of the human mandible with adequate details to acquire clinically valuable results. The second major interest in this study was to investigate the stress distribution induced by different angles of MRM relative to the ORL to provide orthodontists with a clear clinical reference. Although studies have addressed the angulation of mini-screws relative to the bone surface, most of these studies relied on simplified bone blocks instead of actual clinical data in their simulation of 3D models. Therefore, the results of such studies could be difficult to apply to different placement sites, especially if we take into consideration the differences in the anatomy, density and thickness of bone in different intraoral locations. These differences affect the diameter of mini screws that inserted interradicular or extra-alveolar areas. The mini-screw diameter could play a significant role in the failure load in both torque and shear resistance (Smith *et al.*, 2015; Sfondrini *et al.*, 2018).

The mini-screws used in this study were 2 mm in diameter and 10 mm in length. These dimensions can ensure better stress distribution around the mini-screw, especially at the mini-screw neck. A previous study showed that an increased mini-screw diameter enhanced the primary stability of the mini-screw (Alrbata *et al.*, 2014). In addition, a higher implant diameter gives enough strength to the mini screw to avoid fracture during placement or loading. Furthermore, the mini-screw length chosen in this study can ensure safe and successful placement (Lemieux *et al.*, 2011).

It is important to mention that the bone in this study was considered to be homogeneous isotropic, and properties of cortical bone were assigned to the model since the cortical

bone largely rules the transmission of force from the mini-screw to the bone, and the role of trabecular bone thickness and density was inconsequential (Stahl *et al.*, 2009; Suzuki *et al.,* 2011, 2011; Liu *et al.*, 2012). Moreover, Alrbata *et al.* (2014) reported that Von Mises stress decreases as cortical bone thickness increases, and that trabecular bone has an important role in absorbing stress when cortical bone thickness is less than or equal to 1 mm. Nevertheless, this role waned gradually and almost disappeared when the cortical bone thickness exceeded 2 mm (Alrbata *et al.*, 2014). It is worth mentioning that the cortical bone thickness in the retromolar pad area ranges between 3 mm to 5 mm (Nucera *et al.*, 2019).

Von Mises Stresses Induced by Different MRM Angulations

Von Mises stresses at angles of 0°, 15° and 30° were distributed throughout the bone. At 45° and 60°, the generated stresses were concentrated at the contact area between the MRM and the surrounding bone. This result was in accordance with that of Alrbata *et al.* (2014) who found that stresses concentrated only in small contact areas between the mini-screw and the bone. In addition, when the MRM was inserted parallel to the ORL (i.e. at an angle of 0°), the stresses were less than when the angle with the ORL increased, and this was true in cases of different MRM materials. The parallel insertion of an MRM with the ORL reduced the fulcrum of force, which decreased the bending moment generated in the contact area between the MRM and the surrounding bone. In other words, when the angulation of the MRM increases, the fulcrum of force and related bending moment also increase. This increase in the bending moment allowed for more stress to be induced in the contact area between the MRM and surrounding bone. This result aligns with the findings of Ardani *et al.* (2024) who reported that as the angulation increases, the stress on the mini screw also increases. They attributed this to the increased lever arm of the mini-screw, which reduces its anchorage resistance and predisposes it to failure (Ardani *et al.*, 2024). Thus, we recommend parallel angulation if clinicians wish to obtain better stability with MRM. Nevertheless, orthodontists may find it difficult to apply force on MRM inserted parallel to the ORL. Therefore, the insertion of MRM at angles of 15° and 30° are suitable alternatives. It is important to mention that the shape of the retromolar pad area is different between individuals depending on the size of the mandible, the location of the mandibular third molar and the time of their extraction. Therefore, when the space in the retromolar pad area is not sufficient for certain angulations (45° and 60°), smaller angles (15° and 30°) could be a more feasible option.

Von Mises Associated with Different MRM Materials

Regarding materials, there was no significant difference in the Von Mises stresses among the tested materials for angles of 0°, 15° and 30°. This result agreed with those of Singh *et al.* (2012), who reported that there was no difference in stresses that transferred to the bone around SS and Ti mini screws. As mentioned before, the Von Mises stress equivalently transferred to the surrounding bone at 0°, 15° and 30° angles, which explained why there was no difference in the Von Mises stress among the different materials at these angles. However, at angles of 45° and 60°, when stresses concentrated at the contact areas between the MRM and surrounding bones, the SS MRM generated the highest stresses, followed by Ti alloy MRM and pure Ti MRM. This result was consistent with that of Singh *et al.* (2012) who found that the stress generated at the SS mini-screw is higher than that at the Ti alloy mini-screw. This finding was attributed to the high modulus of elasticity of SS compared to that of pure and Ti alloys.

Interestingly, all values of Von Mises stress in this study were less than the yield strength of cortical and trabecular bones. This might imply that no damage in the bone is expected to occur from orthodontic force-

induced stresses. The values of Von Mises stress reported in this study ranged between 5.184 and 8.812 MPa, which are far lower than other study values (Suzuki *et al.,* 2011; Alrbata *et al*., 2014; Perillo *et al*., 2015), where Von Mises stresses ranged between 20 MPa and 382 MPa. One of the reasons behind these differences is that previous studies have adopted simplified bone models that do not rely on actual clinical 3D models and may be related to the mini-screw diameter. Since the diameter of MRM in our study was 2 mm, the stress was distributed to larger contact areas, while in the studies by Suzuki *et al.* (2011) and Perillo *et al.* (2015), mini-screws were 1.3 mm in diameter and 9 mm in length and 1.6 mm in diameter and 8 mm in length, respectively.

Displacement Induced by Different MRM Angulations and Materials

When the angle of insertion of the MRM increases, the displacement of the MRM inside the bone also increases. The increase in angulation leads to an upsurge in the bending moment that affects MRM, which leads to the movement of MRM through the bone. In terms of materials for the same angle, pure Ti MRM resulted in higher displacement compared to those made of Ti alloy and SS. This result was related to the fact that pure Ti has a lower modulus of elasticity, which made it more strongly subjected to dislocation compared to the Ti alloy and SS. Again, this result was in accordance with that of Singh *et al.* (2012).

Moreover, the amount of displacement did not exceed 0.7 μm, which was consistent with the findings of Nienkemper *et al.* (2014), who stated that a primary displacement less than 0.1 mm rarely causes any clinical concerns. Although the difference in the MRM displacements was not clinically significant, the insertion of MRM at 0° with the ORL generated the least MRM displacements and stresses in the surrounding bone compared to other angles. This angulation factor might have a vital impact on secondary displacement that occurs through a time of treatment due bone remodelling (Nienkemper *et al*., 2014).

Limitations of the Study

In our study, we did not simulate the periodontal ligament (PDL) in the 3D model of the mandible due to the insertion of mini-implants (MRM) in areas distant from tooth roots. Choi *et al.* (2016) found minimal Von Mises stresses at the roots and PDLs during force application, regardless of insertion angle, in a study focusing on mini-screws inserted intra-radicular areas, differing from our extra-alveolar insertion approach.

Furthermore, our model assumed uniform properties for cortical bone, primarily due to the inherent difficulty in precisely distinguishing between cortical and trabecular bone in our imaging data. While acknowledging this simplification and its limitation in representing bone as homogeneous, it allowed us to focus on comparing stress distributions within the retromolar pad area across various mini-screw angles and materials.

However, this simplification presents a constraint in our study, given the inherent structural differences between cortical and trabecular bone in reality. Future research endeavours should strive to refine segmentation techniques or utilise advanced imaging modalities to accurately differentiate and assign distinct material properties to each bone type. By doing so, we can enhance the accuracy of finite element models, offering a more nuanced understanding of the mechanics at the bone-implant interface.

CONCLUSION

This study found that increasing the insertion angle of MRM relative to the ORL increases stress and displacement in the surrounding bone. SS MRM showed the highest Von Mises stress at larger angles (45° and 60°), while pure Ti MRM had the greatest displacement. However, all Von Mises stress values were below the bone's yield

strength, indicating no risk of bone damage under orthodontic forces. Some clinical recommendations based on the present study are: (a) A parallel insertion (0° angle) is ideal for reducing stress and displacement, but angles of 15° and 30° are acceptable if a 0° insertion is impractical; and (b) SS MRM provides better stability at higher angles.

REFERENCES

Al-Hafidh NN, Al-Khatib AR, Al-Hafidh NN (2020). Assessment of the cortical bone thickness by CT-scan and its association with orthodontic implant position in a young adult Eastern Mediterranean population: A cross-sectional study. *Int Orthod*, **18**(2): 246–257. https://doi.org/10.1016/j.ortho.2020.02.001

Al-Hafidh NN, Al-Khatib AR, Al-Hafidh NN (2022). Cortical bone thickness and density: Inter-relationship at different orthodontic implant positions. *Clin Investig Orthod*, **81**(1): 20–27. https://doi.org/10.1080/13440241.2021.2024013

Alrbata RH, Yu W, Kyung HM (2014). Biomechanical effectiveness of cortical bone thickness on orthodontic microimplant stability: An evaluation based on the load share between cortical and cancellous bone. *Am J Orthod Dentofacial Orthop*, **146**(2): 175–182. https://doi.org/10.1016/j.ajodo.2014.04.018

AlSamak S, Al-Hafidh NN, Al-Khatib AR (2022). Evaluation of potential mini-implant insertion sites for maxillary skeletal expander: A computerized tomography study. *Clin Investig Orthod*, **81**(1): 34–42. https://doi.org/10.1080/13440241.2022.2035065

Ardani IGAW, Hariati IVD, Nugraha AP, Narmada IB, Syaifudin A, Perkasa IBA *et al.* (2024). Comparison of biomechanical performance of titanium and polyaryletheretherketone miniscrews at different insertion angles: A finite element analysis. *J Orthod Sci*, **13**: 13. https://doi.org/10.4103/jos.jos_102_23

Barros SE, Vanz V, Chiqueto K, Janson G, Ferreira E (2021). Mechanical strength of stainless steel and titanium alloy mini-implants with different diameters: An experimental laboratory study. *Prog Orthod*, **22**(1): 9. https://doi.org/10.1186/s40510-021-00352-w

Baumgaertel S, Hans MG (2009). Assessment of infrazygomatic bone depth for miniscrew insertion. *Clin Oral Implants Res*, **20**(6): 638–642. https://doi.org/10.1111/j.1600-0501.2008.01691.x

Carter DR, Hayes WC (1977). The compressive behavior of bone as a two-phase porous structure. *J Bone Joint Surg Am*, **59**(7): 954–962. https://doi.org/10.2106/00004623-197759070-00021

Chandhoke TK, Nanda R, Uribe FA (2015). Clinical applications of predictable force systems. Part 2: Miniscrew anchorage. *J Clin Orthod*, **49**(4): 229–239.

Choi SH, Kim SJ, Lee KJ, Sung SJ, Chun YS, Hwang CJ (2016). Stress distributions in peri-miniscrew areas from cylindrical and tapered miniscrews inserted at different angles. *Korean J Orthod*, **46**(4): 189–198. https://doi.org/10.4041/kjod.2016.46.4.189

Cozzani M, Nucci L, Lupini D, Dolatshahizand H, Fazeli D, Barzkar E *et al.* (2020). The ideal insertion angle after immediate loading in Jeil, Storm, and Thunder miniscrews: A 3D-FEM study. *Int Orthod*, **18**(3): 503–508. https://doi.org/10.1016/j.ortho.2020.03.003

Kuroda S, Inoue M, Kyung H M, Koolstra JH, Tanaka E (2017). Stress distribution in obliquely inserted orthodontic miniscrews evaluated by three-dimensional finite-element analysis. *Int J Oral Maxillofac Implants*, **32**(2): 344–349. https://doi.org/10.11607/jomi.5061

Lee J, Kim JY, Choi YJ, Kim KH, Chung CJ (2013). Effects of placement angle and direction of orthopedic force application on the stability of orthodontic miniscrews. *Angle Orthod*, **83**(4): 667–673. https://doi.org/10.2319/090112-703.1

Lemieux G, Hart A, Cheretakis C, Goodmurphy C, Trexler S, McGary C *et al.* (2011). Computed tomographic characterization of mini-implant placement pattern and maximum anchorage force in human cadavers. *Am J Orthod Dentofacial Orthop*, **140**(3): 356–365. https://doi.org/10.1016/j.ajodo.2010.05.024

Liu TC, Chang CH, Wong TY, Liu JK (2012). Finite element analysis of miniscrew implants used for orthodontic anchorage. *Am J Orthod Dentofacial Orthop*, **141**(4): 468–476. https://doi.org/10.1016/j.ajodo.2011.11.012

Magkavali-Trikka P, Emmanouilidis G, Papadopoulos MA (2018). Mandibular molar uprighting using orthodontic miniscrew implants: A systematic review. *Prog Orthod*, **19**: 1. https://doi.org/10.1186/s40510-017-0200-2

Mecenas P, Espinosa DG, Cardoso PC, Normando D (2020). Stainless steel or titanium mini-implants? *Angle Orthod*, **90**(4): 587–597. https://doi.org/10.2319/081619-536.1

Migliorati M, Benedicenti S, Signori A, Drago S, Barberis F, Tournier H *et al.* (2012). Miniscrew design and bone characteristics: An experimental study of primary stability. *Am J Orthod Dentofacial Orthop*, **142**(2): 228–234. https://doi.org/10.1016/j.ajodo.2012.03.029

Migliorati M, Drago S, Schiavetti I, Olivero F, Barberis F, Lagazzo A *et al.* (2015). Orthodontic miniscrews: An experimental campaign on primary stability and bone properties. *Eur J Orthod*, **37**(5): 531–538. https://doi.org/10.1093/ejo/cju081

Nienkemper M, Handschel J, Drescher D (2014). Systematic review of mini-implant displacement under orthodontic loading. *Int J Oral Sci*, **6**(1): 1–6. https://doi.org/10.1038/ijos.2013.92

Nienkemper M, Pauls A, Ludwig B, Wilmes B, Drescher D (2012). Multifunctional use of palatal mini-implants. *J Clin Orthod*, **46**(11): 1679–1686.

Nowak R, Olejnik A, Gerber H, Frątczak R, Zawiślak E (2021). Comparison of tooth- and bone-borne appliances on the stress distributions and displacement patterns in the facial skeleton in surgically assisted rapid maxillary expansion: A finite element analysis (FEA) study. *Materials (Basel)*, **14**(5): 1152. https://doi.org/10.3390/ma14051152

Nucera R, Bellocchio AM, Oteri G, Farah AJ, Rosalia L, Giancarlo C *et al.* (2019). Bone and cortical bone characteristics of mandibular retromolar trigone and anterior ramus region for miniscrew insertion in adults. *Am J Orthod Dentofacial Orthop*, **155**(3): 330–338. https://doi.org/10.1016/j.ajodo.2018.04.025

Omar A, Ishak MI, Harun MN, Sulaiman E, Kasim NHA (2011). Effects of different angulation placement of mini-implant in orthodontic. *Appl Mech Mater*, **121–126**: 1214–1219. https://doi.org/10.4028/www.scientific.net/AMM.121-126.1214

Papadopoulos MA, Tarawneh F (2007). The use of miniscrew implants for temporary skeletal anchorage in orthodontics: a comprehensive review. *Oral Surg Oral Med Oral Pathol Oral Radiol Endod*, **103**(5): e6–e15. https://doi.org/10.1016/j.tripleo.2006.11.022

Papageorgiou SN, Zogakis IP, Papadopoulos MA (2012). Failure rates and associated risk factors of orthodontic miniscrew implants: A meta-analysis. *Am J Orthod Dentofacial Orthop*, **142**(5): 577–595. https://doi.org/10.1016/j.ajodo.2012.05.016

Park HS, Lee Y J, Jeong SH, Kwon TG (2008). Density of the alveolar and basal bones of the maxilla and the mandible. *Am J Orthod Dentofac Orthop*, **133**(1): 30–37. https://doi.org/10.1016/j.ajodo.2006.01.044

Paul P, Mathur AK, Chitra P (2021). Stress distribution patterns in mini-implant and bone in the infra-zygomatic crest region at different angulations: A finite element study. *J World Fed Orthod*, **10**(1): 29–34. https://doi.org/10.1016/j.ejwf.2020.11.004

Perillo L, Jamilian A, Shafieyoon A, Karimi H, Cozzani M (2015). Finite element analysis of miniscrew placement in mandibular alveolar bone with varied angulations. *Eur J Orthod*, **37**(1): 56–59. https://doi.org/10.1093/ejo/cju006

Poletti L, Silvera AA, Ghislanzoni LTH (2013). Dentoalveolar class III treatment using retromolar miniscrew anchorage. *Prog Orthod*, **14**: 7. https://doi.org/10.1186/2196-1042-14-7

Sfondrini MF, Gandini P, Alcozer R, Vallittu PK, Scribante A (2018). Failure load and stress analysis of orthodontic miniscrews with different transmucosal collar diameter. *J Mech Behav Biomed Mater*, **87**: 132–137. https://doi.org/10.1016/j.jmbbm.2018.07.032

Sidhu M, Chugh VK, Dmello K, Mehta A, Chugh A, Tandon P (2020). Evaluation of stress pattern caused by mini-implant in mandibular alveolar bone with different angulations and retraction forces: A three-dimensional finite element study. *Turk J Orthod*, **33**(3): 150–156. https://doi.org/10.5152/TurkJOrthod.2020.19109

Singh S, Mogra S, Shetty VS, Shetty S, Philip P (2012). Three-dimensional finite element analysis of strength, stability, and stress distribution in orthodontic anchorage: a conical, self-drilling miniscrew implant system. *Am J Orthod Dentofacial Orthop*, **141**(3): 327–336. https://doi.org/10.1016/j.ajodo.2011.07.022

Sivamurthy G, Sundari S (2016). Stress distribution patterns at mini-implant site during retraction and intrusion: A three-dimensional finite element study. *Prog Orthod*, **17**: 4. https://doi.org/10.1186/s40510-016-0117-1

Smith A, Hosein YK, Dunning CE, Tassi A (2015). Fracture resistance of commonly used self-drilling orthodontic mini-implants. *Angle Orthod*, **85**(1): 26–32. https://doi.org/10.2319/112213-860.1

Stahl E, Keilig L, Abdelgader I, Jager A, Bourauel C (2009). Numerical analyses of biomechanical behavior of various orthodontic anchorage implants. *J Orofac Orthop*, **70**(2): 115–127. https://doi.org/10.1007/s00056-009-0817-y

Sugawara Y, Kuroda S, Tamamura N, Takano-Yamamoto T (2008). Adult patient with mandibular protrusion and unstable occlusion treated with titanium screw anchorage. *Am J Orthod Dentofacial Orthop*, **133**(1): 102–111. https://doi.org/10.1016/j.ajodo.2006.06.020

Suzuki A, Masuda T, Takahashi I, Deguchi T, Suzuki O, Takano-Yamamoto T (2011). Changes in stress distribution of orthodontic miniscrews and surrounding bone evaluated by 3-dimensional finite element analysis. *Am J Orthod Dentofacial Orthop*, **140**(6): e273–e280. https://doi.org/10.1016/j.ajodo.2011.06.025

Wang S, Bing L, Park HS (2021). Optimal microimplant sites in the mandibular retromolar area: Mesh analysis of cortical bone thickness and density in CBCT images. *Int J Morphol*, **39**(3): 907–914.

World Medical Association (WMA) (2013). *WMA Declaration of Helsinki - Ethical Principles for Medical Research Involving Human Subjects. 64th WMA General Assembly, Fortaleza, Brazil, October 2013.* Retrieved 30 April 2024, from https://www.wma.net/wp-content/uploads/2024/10/DoH-Oct2013.pdf

Yanagita T, Kuroda S, Takano-Yamamoto T, Yamashiro T (2011). Class III malocclusion with complex problems of lateral open bite and severe crowding successfully treated with miniscrew anchorage and lingual orthodontic brackets. *Am J Orthod Dentofacial Orthop*, **139**(5): 679–689. https://doi.org/10.1016/j.ajodo.2009.07.023

Yeon BM, Lee NK, Park JH, Kim JM, Kim SH, Kook YA (2022). Comparison of treatment effects after total mandibular arch distalization with miniscrews vs ramal plates in patients with Class III malocclusion. Am *J Orthod Dentofacial Orthop*, **161**(4): 529–536. https://doi.org/10.1016/j.ajodo.2020.09.040